Crystallization behaviour of random block copolymers of poly(butylene terephthalate) and poly(tetramethylene ether glycol)

R. M. Briber* and E. L. Thomas
Polymer Science and Engineering Department, University of Massachusetts, Amherst, MA 01003, USA
(Received 19 January 1984; revised 5 April 1984)

The morphology and crystallization behaviour of random block copolymers of poly(butylene terephthalate) and poly(tetramethylene ether glycol) have been investigated. Single crystals have been grown in thin films crystallized from the melt. Well defined lamellae, exhibiting (*hk*O) single crystal electron diffraction patterns have been observed in copolymers containing down to 49 wt% (0.83 mole fraction) poly(butylene terephthalate). WAXS and electron diffraction support a model of a relatively pure poly(butylene terephthalate) crystal core with the poly(tetramethylene ether glycol) (soft segment) sequences and short hard segments being rejected to the lamellar surface and the soft segment rich matrix. The lateral dimensions of the lamellae are determined by the number of hard segment sequences long enough to traverse the stable crystal size at the crystallization temperature. This leads to an initial population of crystals formed at T_c and a second set of smaller crystals that grow from the short hard segment sequences upon cooling to room temperature. The result is fractionation by sequence length due to a coupling of the sequence distribution with the stable crystal size at the crystallization temperature.

(Keywords: copolymer; morphology; poly(butylene terephthalate); single crystals; electron microscopy; polyether–polyester)

INTRODUCTION

The polyether–polyesters examined in this study are random block copolymers containing crystallizable hard segments and elastomeric, amorphous soft segments. By random block copolymer it is meant that polyether–polyesters are multiblock copolymers of the $\{AB\}_n$ type with A and B each representing a length of chain of a different polymer. Random block copolymers are distinguished from random copolymers because one of the starting components (the soft segment) used in the copolymerization reaction is not a single repeat unit but starts as an oligomer, usually of 1000–4000 molecular weight. The lengths of the sequences of A and B units follow a geometrical distribution, hence the block length varies considerably, with the average being determined by the molar composition of the sample. One of the blocks is termed the hard segment because it is a rigid, high modulus plastic at the desired use temperature. The other block is called the soft segment and is an elastomer at the use temperature. Microphase separation occurs with the formation of hard and soft segment rich domains. The hard segment domains or crystallites act as physical crosslinks for the soft segment material at low hard segment content giving the polyether–polyesters properties similar to a classical crosslinked rubber without the use of covalent crosslinks. At high hard segment content the soft segment acts as a toughening agent for the hard segment material. The morphology of polyether–polyesters, indeed of all random block copolymers, is not well understood with most of the morphological insight being drawn from such indirect experiments as dynamical mechanical testing and differential scanning calorimetry.

It is generally accepted that the soft segment phase in these polyether–polyesters is a mixture of the soft segment material with short uncrystallized hard segments[1–3]. Only a single glass transition temperature is observed which depends strongly on composition and sample history (which determine the amount of dissolved hard segment in the amorphous phase)[1–3]. The melting of the hard segment domains is observed, near that of the hard segment homopolymer, but depressed somewhat due to small crystal size and defects in the crystals.

The early fundamental structure–property work on polyether–polyesters was done by Cella and has been summarized in a number of articles[1,4,5]. The morphological model presented by Cella consists of interpenetrating crystalline domains. The crystalline domains are lamellar in nature and consist of long polyester (4GT) sequences with the polyether and short 4GT segments rejected to the amorphous phase. Chain folding was postulated for the 4GT crystals by Cella[4]. A short but intriguing paper on the subject of polyether–polyester morphology was published by Seymour *et al.*[6]. The experiments included chemical etching and g.p.c., small-angle light scattering (SALS) and dynamic mechanical experiments. The polymers all exhibited small-angle light scattering patterns characteristic of a spherulitic superstructure. The chemical etching and subsequent g.p.c. revealed a low molecular weight peak that corresponded to a lamellar thickness of 7 to 8 monomer units. Evidence of chain folding was given by a high molecular weight shoulder occurring at twice the molecular weight of the primary peak. This corresponds to chains that traverse the crystal, fold and re-

* Present address: National Bureau of Standards, Gaithersburg, MD 20899, USA.

0032-3861/85/010008-09$03.00

enter the crystal. This high molecular weight peak gradually disappears with longer etching time as the fold surface is slowly degraded. More recent morphological studies on polyether–polyesters were performed by Wegner's group at the University of Freiburg[2,7,8]. In their view the morphology consists of spherulitic aggregations of hard segment lamellae. They postulate that both short and long hard segment sequences are excluded from the crystals with the lamellae being composed almost exclusively of sequences equal to the average length of the hard segment. The long sequences were thought to be excluded because the degree of crystallinity was less than what would be expected if all the sequences greater than or equal to the average length were to crystallize. It is difficult from a physical point of view to understand why all the long hard segment sequences would be excluded from the crystal when some could cooperate in crystallization by folding.

Small-angle X-ray scattering studies have been done, primarily by Bandara and Droscher[9] and Wegner *et al.*[2]. Generally the SAXS results indicate that the copolymers behave similar to homopolymers, with the long period increasing with higher annealing temperatures. In addition to following the long period as a function of crystallization conditions, Bandara and Droscher calculated one dimensional correlation functions, specific inner surface areas, average chord lengths, lamellar thickness, transition zone thickness and the mean squared electron density fluctuation as a function of undercooling and composition. In general the data are consistent as a function of undercooling with the samples crystallized at high temperatures (low undercooling) exhibiting thicker crystals, lower internal surface area and better phase separation. Bandara and Droscher measured the interface width between the two phases and found it to be 0.6 nm for a sigmoidal interface profile model, independent of sample composition and undercooling. The absolute value of interface widths measured by SAXS is dependent on the model chosen. Yet, measurements on polystyrene–polyisoprene block copolymers, known to be incompatible and thought to possess sharp interfaces give a sigmoidal boundary thickness of about 0.4–0.8 nm[10,11]. Therefore the absolute value of 0.6 nm for a system that should have inherently diffuse boundaries appears to be too low.

An interesting crystallization feature observed by Zhu and Wegner[7,8] in isothermally crystallized polyether–polyesters was that at small undercoolings birefringent aggregates can be observed growing scattered throughout the melt. They do not exhibit the usual spherulitic maltese cross extinction pattern in polarized light because they contain only a few relatively large lamellae and therefore do not have a fine enough texture and broad enough range of orientations to exhibit the maltese cross. As a rule these birefringent aggregates stop growing long before they impinge. The matrix surrounding the aggregates never appears to crystallize at T_c even after long times. Yet if the sample is quenched and then annealed at a temperature below the original crystallization temperature new crystals form at the edges of the previous aggregates, indicating there was hard segment material present in the matrix that was unable to crystallize at the original T_c. At the new lower annealing temperature this material crystallizes using the aggregates formed earlier as nucleation sites.

There are a considerable number of papers in the literature dealing with polyether–polyester morphology either directly or indirectly and a number of differing viewpoints have been proposed concerning its nature. It is the aim of this work to use electron microscopy and diffraction in an attempt to understand the basic structural features of polyether–polyesters. In this study the morphology of melt crystallized thin films of polyether–polyesters has been examined. These films exhibit a unique morphology which is discussed and some new ideas regarding the crystallization behaviour of polyether–polyesters and random block copolymers are presented.

EXPERIMENTAL

Materials

The polyether–polyesters examined in this work were based on poly(tetramethylene ether glycol) ($M_n = 1000$) as the soft segment (PTMEG) and poly(butylene terephthalate) as the hard segment (4GT). The polymers were an experimental batch of the polyether–polyesters marketed under the trade name Hytrel by the duPont Company. The samples were supplied by Dr W. H. Buck of the duPont Company. Sample compositions (weight per cent 4GT), mole fraction 4GT and average hard segment length (calculated assuming a most probable distribution) are given in *Table 1*. The 4GT homopolymer studies was Valox 315, supplied by the General Electric Company. Chemical formulas are given in *Figure 1*.

The samples were prepared by a melt condensation reaction between PTMEG, the methyl ester of terephthalic acid and 1,4 butanediol. Details of the synthesis are reviewed in the papers by Cella[1,4] and Wistsiepe[12]. The polyether–polyesters used in this study were chosen because the hard and soft segment sequence distributions and the molecular weight distribution are believed to be

Table 1 Polyether–polyester compositions

Composition (wt% 4GT)	Mole fraction 4GT	Average hard segment length $\bar{N}$
81	0.96	23
73	0.93	15
59	0.88	8
49	0.83	6
43	0.79	5
36	0.74	4

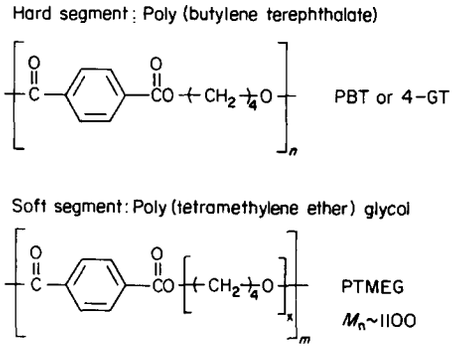

Figure 1 Chemical structures of the polyether–polyester system studied in this work

ideal and follow a most probable distribution. The polymerization is carried out in the melt which is one phase for this molecular weight soft segment. In a recent study by Shih and McKenna the effect of the soft segment molecular weight was studied by dynamic mechanical analysis (d.m.a.) and d.s.c.[13]. For PTMEG molecular weights of 2000 and larger the melt was observed to be opaque during polymerization while for molecular weights of 1000 and below the melt was clear. This observation has also been made by Wolfe[14]. The opacity was taken as evidence of phase separation during polymerization and non-ideal reaction conditions. Non-ideal reaction conditions will lead to sequence distributions that are far from random with one phase rich in hard segment and the other phase rich in soft segment. For soft segment molecular weights less than 2000 the reaction medium is homogeneous leading to a most probable hard segment sequence distribution. Further evidence for random sequence distribution has been presented by Shih[15]. A sample containing 59 wt% hard segment (PTMEG *MW*, 1000) was blended in the melt with pure 4GT homopolymer using a Brabender mixer. At all compositions ranging from 10–90% 4GT two melting points and glass transition temperatures were observed corresponding to the individual components in the blends. The melt was also found to be two-phase with the polyether–polyester and 4GT homopolymer each forming discrete phases as observed by optical microscopy. Although the melt was two phase initially one might expect that at long times the 4GT and polyether–polyester would become one phase as transesterification occurred. If the polyether–polyester copolymer contained large amounts of high hard segment content material, as would be present if the polymerization conditions were non-homogeneous, then two melting points would be expected in the copolymer as seen in the blends. This is not observed. Based on this evidence the conclusion that polyether–polyesters based on PTMEG of 1000 molecular weight (and less) and 4GT have truly random sequence distributions of both hard and soft segments is justified.

Sample preparation

Thin films for melt crystallization experiments were prepared by casting the polyether–polyesters from dilute solution. A 0.075 wt% solution of the polymer was made in hexaflouroisopropanol (HFIP). A freshly cleaved mica sheet was then lightly coated with carbon (~5–10 nm thickness). This prevented the polymer from adhering to the mica in the subsequent crystallization step. The mica was dipped into the polymer solution and the excess solution wiped off the bottom of the mica with filter paper. The solvent was then quickly evaporated by placing the mica on a warm hot plate in a hood. If the solvent was not evaporated rapidly the film produced was not homogeneous and contained holes and thickness variations. The mica sheet was placed in a hot stage which was either under N_2 purge or inside a N_2-filled glove bag. The polymer film was melted and held at 250°C for 5 min and then quenched to the desired crystallization temperature (T_c). The polymer was kept at T_c for 4 h and subsequently quenched to room temperature. The film was floated off the mica onto distilled water and picked up on electron microscopic grids.

Electron microscopy

Transmission electron microscopy was performed using a JEOL 100 CX transmission electron microscope equipped with a scanning transmission attachment. Since the main limitation in high resolution microscopy of polymers is radiation damage every attempt was made to keep this to a minimum. For bright field (BF) microscopy this entailed focusing in one area and translating to an adjacent area for exposure. To minimize radiation damage during dark field (DF) microscopy the sample was either translated to an adjacent area for exposure or alternatively, with the beam off, the second condenser lens would be excited to bring the beam to crossover. The beam would then be turned on and the image focused and the beam shut off again. Next the condenser lens current would be decreased to a predetermined value to spread the beam for even illumination and a reasonable exposure. The beam would be turned on and the micrograph taken. Only the small central region illuminiated for focusing would be damaged. In all cases exposures were checked to be 0.6–0.8 τ, where τ is the radiation lifetime of the crystal. Dark field microscopy was performed using the tilted beam technique.

Selected area diffraction patterns were obtained by decreasing the strength of the intermediate lens to image the black focal plane of the objective lens. Either a 4 or 8 μm diameter SAD aperture was used.

Microdiffraction patterns were obtained using the STEM attachment and free lens control. In the STEM imaging mode the pre-field of the objective lens is excited allowing the electron beam to be focused into a small probe. The size of the probe determines the resolution attainable and is controlled by the condenser lenses and second condenser lens aperture. A very small probe size (~5 nm) results in a highly convergent beam which gives a convergent beam microdiffraction pattern. This large spread of incident angles in the beam does not affect the image quality in STEM but it results in the microdiffraction spots being very broad with overlap of adjacent reflections. Consequently microdiffraction patterns using more coherent illumination were taken using a beam diameter about 0.5 μm. The main advantage of microdiffraction over selected area diffraction in this application was the ability to take adjacent diffraction patterns without damaging the surrounding area. The 0.5 μm probe size was not a limitation because the features of interest were greater than 1 μm in size. Scanning transmission electron microscopy as applied to polymers has been discussed in the literature by Low *et al.*[16] and by Thomas *et al.*[17–19].

Differential scanning calorimetry

Differential scanning calorimetry (d.s.c.) was performed with a computer controlled Perkin Elmer DSC-2. Temperature scale and thermal input were calibrated using an indium standard. All d.s.c. scans were carried out at a scan rate of 20°C min^{-1}. Sample size was ~10 mg. The d.s.c. scans presented are all normalized to 1 mg sample size.

Wide-angle X-ray scattering

Wide-angle X-ray scattering samples were prepared by melt pressing 1.0 mm thick samples and subsequently crystallizing them at the desired temperature. Diffractometry was done on a Siemens D-500 diffractometer. Incident slits defining an angle of 0.3° were generally used.

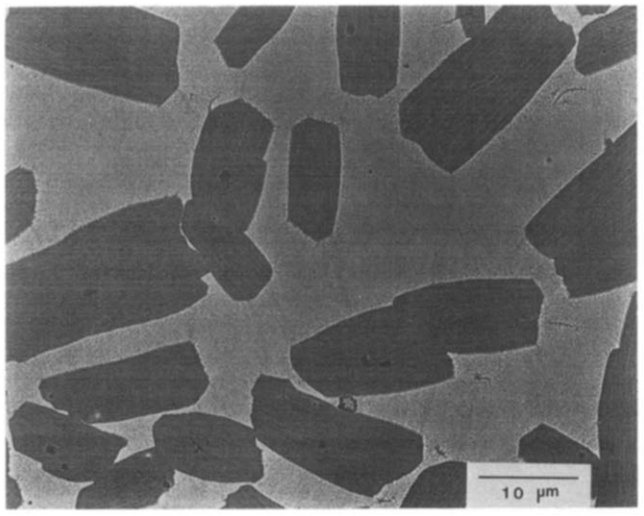

Figure 2 Low magnification BF *TEM* micrograph of a melt crystallized 73% by weight hard segment polyether–polyester film

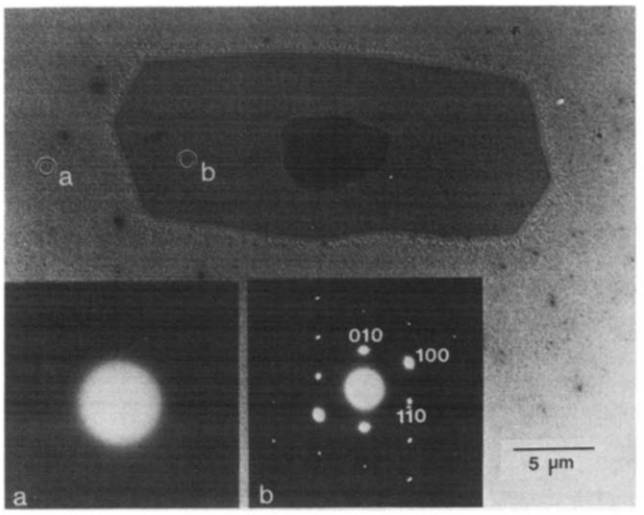

Figure 3 BF *TEM* micrograph and associated microdiffraction patterns from 73% by weight hard segment polyether–polyester film. (a) Microdiffraction pattern from matrix; (b) microdiffraction patterns from lamella

Receiving slits were 0.3° and 0.05°. The 2θ scan rate was $1° \text{ min}^{-1}$. Samples were run in reflection.

RESULTS AND DISCUSSION

Electron microscopy

Three different polymers were studied by melt crystallizing thin films and subsequently examining them in the electron microscope: pure 4GT homopolymer (Valox 315), 73% hard segment polyether–polyester, and a 49% hard segment polyether–polyester. The 73% content sample was studied most thoroughly and will be discussed in the most detail.

Films crystallized at low undercoolings ($\Delta T \simeq 10°$–15°C) were found to have single crystal lamellae growing in them. Isolated single crystals grown in thin films from the melt have been previously reported for homopolymers, without much discussion[20]. *Figure 2* is a low magnification bright field electron micrograph of a 73% hard segment content film crystallized at 200°C ($\Delta T \simeq 15$°C, $T_m \simeq 215$°C[21,22], see also the d.s.c. data presented in this work). Many relatively large (25 μm long) single lamellae can be observed growing in the plane of the film. The lamellae appear to be uniform in thickness except for an occasional small overgrowth near the centre. *Figure 3* is slightly higher magnification micrograph of a single lamella and associated microdiffraction patterns from the lamella and the surrounding matrix. The lammella gives a strong single crystal diffraction pattern while the matrix shows only diffuse amorphous scattering. *Figure 4* is an indexed electron diffraction pattern from a single lamella in a 73% hard segment content film. The pattern indexes to the alpha unit cell of 4GT[23–27]. Similar patterns were also obtained from films of the 4GT homopolymer and the 49% hard segment polymer. The d-spacings measured were found to be independent of soft segment concentration. The beta polymorph is reported to only appear under stress in the homopolymer[23–27] and would not be expected in quiescently crystallized films. The fact that the crystals give rise to (*hk*0) type reflections indicates that the lamellar surface coincides with the $\underset{\sim}{a}^*$–$\underset{\sim}{b}^*$ plane of the unit cell. The $\underset{\sim}{c}$ axis, and hence the chain direction, is perpendicular to the $\underset{\sim}{a}^*$–$\underset{\sim}{b}^*$ plane and the lamellar surface. Since the unit cell is triclinic the directions of $\underset{\sim}{a}, \underset{\sim}{b}, \underset{\sim}{c}$ do not coincide with $\underset{\sim}{a}^*, \underset{\sim}{b}^*, \underset{\sim}{c}^*$ and the $\underset{\sim}{a}$ axis is not in the plane of the film. The crystal habit of 4GT has been clearly observed as a result of these morphological investigations on polyether–polyesters. For a complete discussion see Ref. 28. *Figure 5* is a low magnification BF micrograph of a 49% hard segment film crystallized at 190°C ($\Delta T \simeq 15$°C, $T_m \simeq 205$°C[21,22]. Small lamellae can be observed throughout the film. The largest lamellae are only about 10 μm in length, in contrast to the much larger crystals in the 73% hard segment film. Another interesting

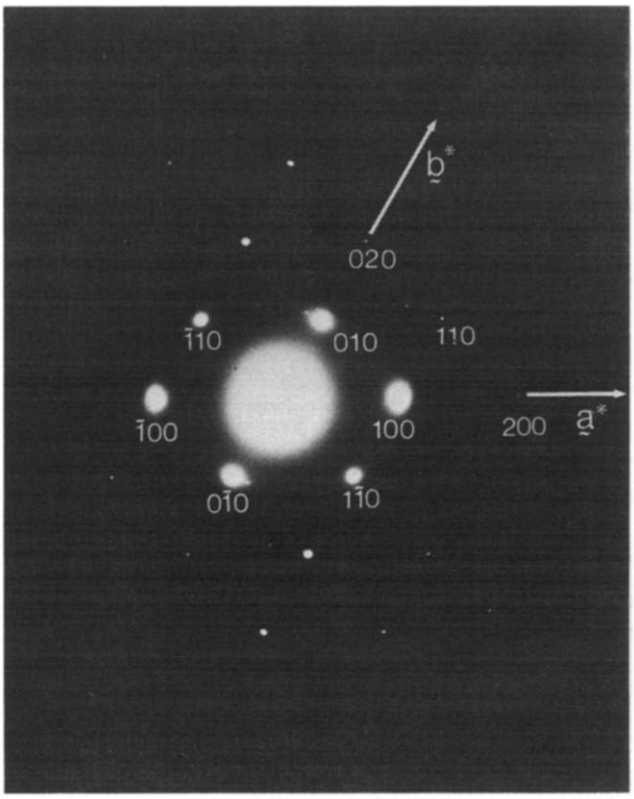

Figure 4 Indexed electron diffraction pattern from a lamellae in a 73% by weight polyether–polyester film. Pattern indexes with the α form of 4GT

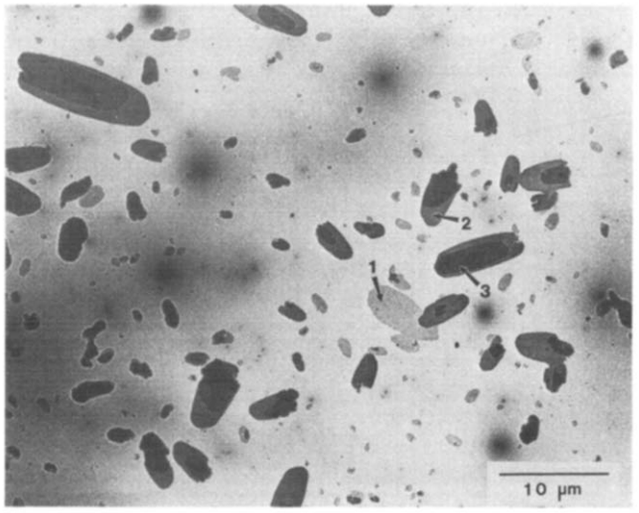

Figure 5 Low magnification BF *TEM* micrograph at a melt crystallized 49% by weight hard segment polyether–polyester film. Arrows indicate mono-, bi- and tri-layer crystals

feature in the 49% film is that not all the lamellae are the same thickness. Definite step changes in contrast corresponding to integral layers of lamellae can be observed. Indicated by the arrows and numbers in *Figure 5* are mono-, bi- and tri-layers. Virtually all of the large crystals are either bilayers or thicker with the different layers following the same growth front. This is not seen in the 73% content films where the crystals appear mostly as single monolayers. Once a chain exits the hard segment crystal in the 49% hard segment sample it appears to be just as likely to re-enter the original lamellae as it is to enter one directly adjacent. In the 73% hard segment sample the smaller amount of soft segment causes it to be more favourable for the chain to re-enter the same crystal.

An attempt was made to grow single lamellae in films of 4GT homopolymer but the nucleation density was too high to allow the identification of isolated crystals. Single crystal diffraction patterns were obtained but the growth fronts and overall shape of the crystals were not discernible.

Figure 6 is a pair of dark field micrographs of the same crystal using the (100) and (010) reflections to form the images, respectively, in a 73% hard segment film (T_c=200°C). The most striking aspect of the crystal is that it appears to be divided into strips parallel to (010) planes. The strips are generally about 0.25–1.0 μm in width and often run the entire length of the crystal. *Figure 7* is a bright field—(100) dark field pair of micrographs of the same area of a 73% hard segment crystal. The strip boundaries observed in dark field appear to be cracks in the crystal in the bright field micrograph. A possible explanation for the cracks is that the crystal grows as a single unit at the high (200°C) crystallization temperature but breaks up on cooling to room temperature due to the larger thermal contraction of the amorphous matrix surrounding the crystal. This would indicate that the mechanical strength is poor between the (010) planes and the crystal cracks easily parallel to these planes. The (010) plane has the largest d-spacing in the (*hk*0) unit cell projection and might be expected to be an easy cleavage plane. Another possible explanation is that any chain folding that might be present occurs along the (010) planes which would lead to easy crack propagation parallel to the (010) planes. While (010) folding is indicated by the sides of the crystals being (010) planes, the (100) and (1$\bar{1}$0) facets present at the ends of the crystals implies folding parallel to the (100) and (1$\bar{1}$0) planes in the regions (sectors) defined by these facets. As previously mentioned, evidence for chain folding exists from the g.p.c. work done by Seymour *et al.*[6]. It is interesting to note that the cracks are not observed in the smaller crystals grown in the 49% hard segment content films.

Another explanation for the strip boundaries observed in the dark field micrographs of the 73% hard segment crystals is that they correspond to boundaries between fold domains. This explanation does not hold up to closer scrutiny because the diffraction contrast features associated with fold domain boundaries would be expected to disappear with radiation damage[29,30]. These 'boundaries' remain after the crystal has been completely damaged. In addition the contrast features associated with the strip boundaries do not shift with defocus of the electron microscope objective lens while for fold sector boundaries they would be expected to shift[29,30].

No clear evidence of sectorization or sector boundaries was observed by bright or dark field electron microscopy. As mentioned previously the cracks observed often run

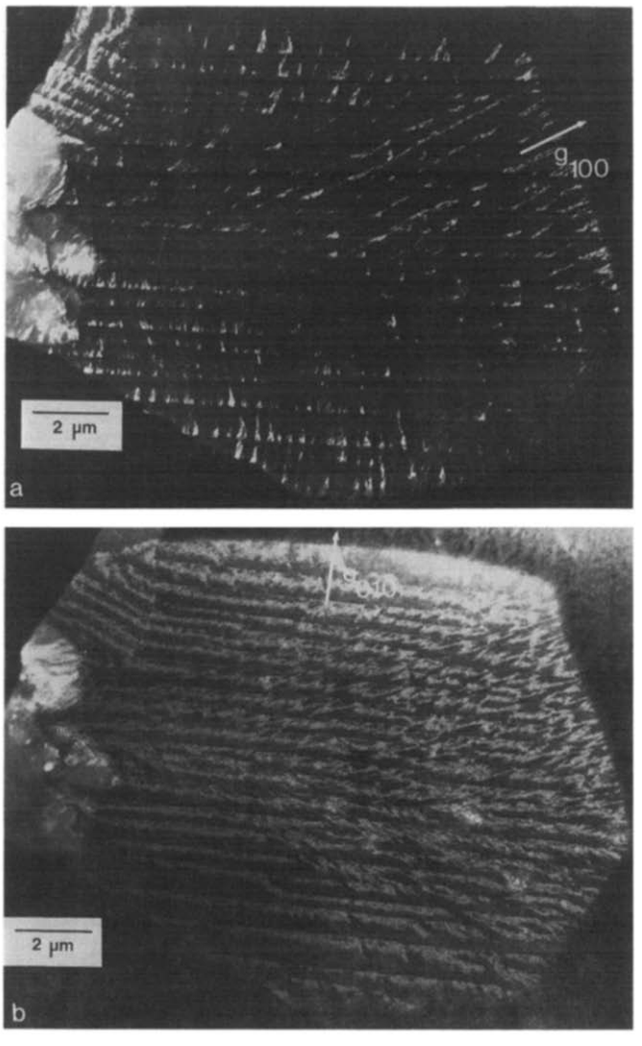

Figure 6 Pair of dark field micrographs of the same crystal in a 73% polyether–polyester hard segment film. (a) Image formed using the (100) reflection; (b) image formed using the (010) reflection

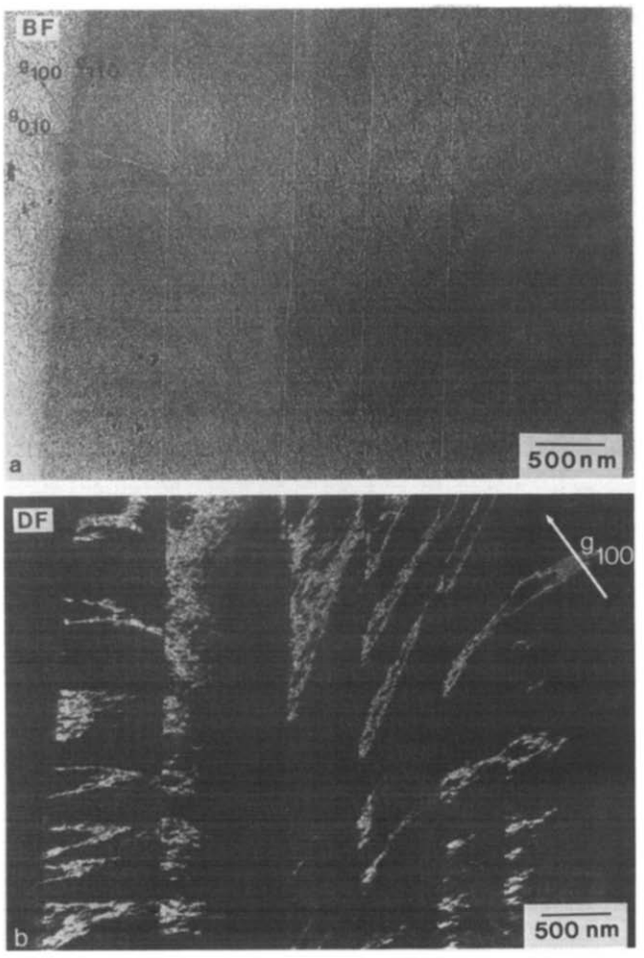

Figure 7 Bright field-dark field pair of micrographs of a 73% hard segment polyether–polyester lamella. (a) Bright field micrograph, note the presence of cracks running parallel to the (010) planes; (b) dark field micrograph, note the discontinuity in the diffracting regions at the crack boundaries

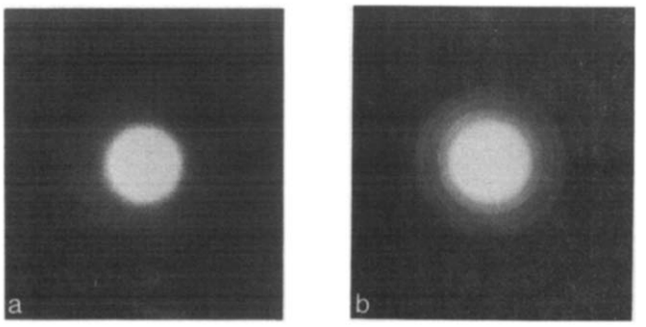

Figure 8 Electron diffraction patterns from the matrix material in a 73% polyether–polyester and hard segment film. (a) Immediately after crystallization; (b) after storage for 3 months at room temperature. Note the presence of polycrystalline rings in (b)

the entire length of the crystals whereas a change in the crack propagation behaviour is usually expected upon traversing from one fold sector to another. Similar crystal faceting behaviour with only poorly defined sectorization has been observed in solution grown nylon-6,6 crystals[31].

When the films were initially examined, the matrix surrounding the crystals was amorphous as indicated by the microdiffraction pattern in *Figure 3*. The films were then stored at room temperature for about 3 months and re-examined. It was found that the matrix had partially crystallized. *Figure 8* is a pair of electron diffraction patterns from the matrix material of a 73% hard segment film, taken with a few hours after quenching from T_c and after about 3 months at room temperature. The polycrystalline pattern in *Figure 8b* corresponds to the alpha form of 4GT indicating that there was a significant amount of hard segment material present in the matrix that was unable to crystallize at T_c. *Figure 9* is a dark field micrograph of the matrix material taken using the polycrystalline rings to form the dark field image. The edge of a large lamella is seen in the left hand portion of the micrograph. Small 50–20 nm clusters of crystals are visible in the matrix. This observation correlates well with the work of Zhu and Wegner who followed the crystallization of a series of PTMEG (1000)/4GT polyether–polyesters by monitoring the growth of lamellar aggregates (hedrites) by optical microscopy as a function of time at a given T_c[7,8]. They observed that the hedrites stopped growing at a given T_c long before impingement. Upon cooling to a lower T_c the hedrites would commence growing again at the edges of the original aggregates. This is analogous to our thin film crystallization where the lamellae stop growing before the film is completely transformed. After cooling to room temperature short hard segment sequences remaining in the matrix crystallize with time. At the initial high crystallization temperature the stable crystal thickness is large and only relatively long hard segment sequences are able to crystallize. Shorter sequences that are unable to traverse the crystal cannot participate in crystallization. When the sample is

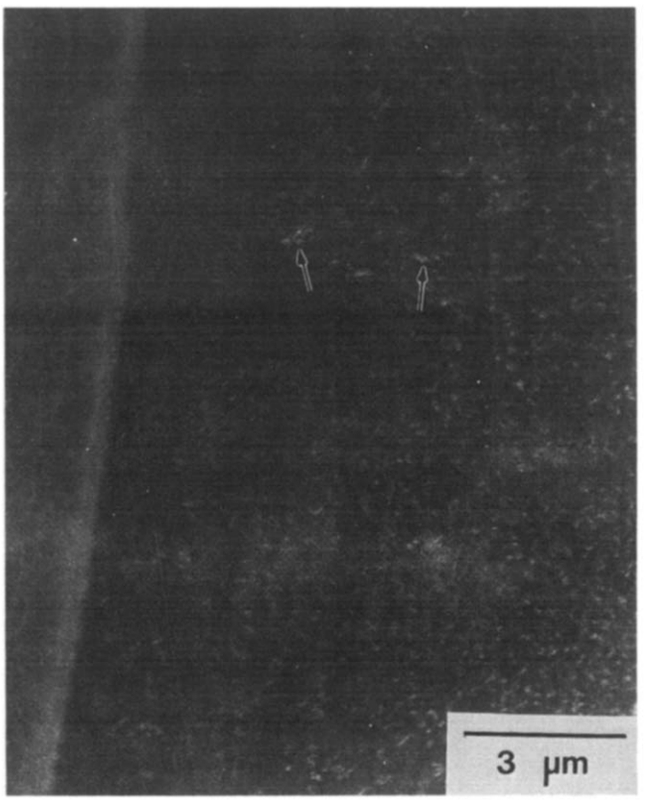

Figure 9 Dark-field micrograph of the matrix in a 73% polyether–polyester hard segment film after storage for 3 months at room temperature. Small aggregations of diffracting crystals are arrowed. Edge of a large lamella is visible in the left hand portion of the micrograph

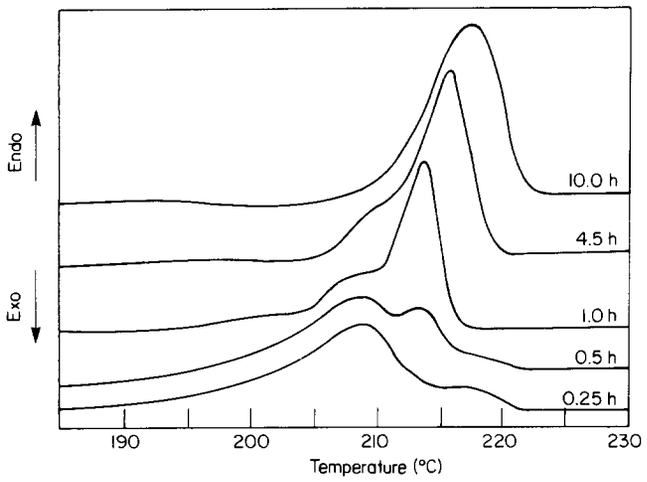

Figure 10 D.s.c. scans of a 73% hard segment polyether–polyester film crystallized at 200°C for various lengths of time

subsequently cooled the stable crystal thickness is less and shorter sequences can then diffuse and crystallize forming the new growth observed at the edges of the hedrites observed by Zhu *et al.* or the small crystals scattered through the matrix seen in this work. This implies that fractionation of the hard segment sequences can occur according to length but not because of incompatibility of different lengths, rather due to coupling of the sequence distribution with the stable crystal size at a given T_c.

Differential scanning calorimetry

D.s.c. scans were run on a 73% hard segment sample crystallized at 200°C for various lengths of time. The samples were melted in the d.s.c. pans in a Mettler hot stage at 250°C for 5 min and then the temperature dropped to 200°C for different times and subsequently quenched to room temperature. Pans were then transferred to the d.s.c. for the measurements. *Figure 10* is a series of scans of samples crystallized for 0.25, 0.5, 1.0, 4.5 and 10 h. At short crystallization times two peaks at about 215° and 207°C are observed. The higher temperature peak arises from the melting of the large lamellae that form at 200°C. The low temperature peak is due to material that crystallizes during the scan and during the quench to room temperature from T_c before the scan. As the crystallization time increases the low temperature peak shrinks while the high temperature peak grows. This is consistent with increased lamellar growth as the crystallization time increases with the consequence of there being fewer long hard segments to crystallize as the small, low melting temperature crystals upon quenching. At 4.5 h at T_c there is only a small shoulder indicative of low temperature crystals and by 10 h only the high melting point material is present. The crystallization of short hard segment sequences in the matrix observed by electron microscopy for thin films indicates that even in the sample crystallized for 10 h there are hard segment sequences present that are not able to crystallize because they are too short to add to the crystals. At room temperature these sequences take weeks to aggregate and crystallize.

The total heat of fusion for both peaks remains relatively constant during crystallization as a function of crystallization time. ΔH_f varies from about 8.5 to 10 cal g^{-1}. This corresponds to the hard segment being about 40% crystalline, using a value of $\Delta H^\circ = 33.5$ cal g^{-1}.[32] If one assumes that all sequences of a minimum length and longer participate in crystallization one can calculate the hard segment length for which 40% of the sequences are equal to or larger from equation (1)

$$N_K^+ = X_{HS}^{K-1} \tag{1}$$

where N_K^+ is the number fraction of hard segment blocks K and longer, X_{HS} is the hard segment mole fraction and K is the block length. Setting N_K^+ equal to 0.40 and X_{HS} equal to 0.93 yields a value of $K = 14$. For the 73% hard segment (0.93 mole fraction) content sample the average sequence length is 15. So it appears that most sequences of about the *average length and greater* participate in crystallization at $T_c = 200$°C. This differs from conclusions drawn by other authors who asserted that only sequences of the average length crystallize with shorter and longer sequences being excluded from the crystal[2,7,8].

Wide-angle X-ray scattering

WAXS diffractometer scans were run on the series of polyether–polyesters and the 4GT homopolymer. *Figure 11* shows the WAXS scans as a function of hard segment content. For samples of 49% hard segment content and higher the $(0\bar{1}1)$, (010) and (100) d-spacings were measured and are given in *Table 2*. The spacings were measured without peak separation or $K_{\alpha 2}$ stripping. All the reflections observed agreed with the alpha form of 4GT. No variation of the unit cell with decreasing hard segment content, within experimental error, was observed. This agrees with the electron diffraction data presented earlier. There does not appear to be any systematic expansion or contraction of the unit cell with decreasing hard segment content as would be expected if appreciable amounts of the soft segment were incorporated into the crystal as defects.

All the data presented so far support a lamellar model of a relatively pure 4GT crystalline core with the PTMEG soft segments rejected to the fold surfaces of the crystal. The striking (*hk*0) electron diffraction patterns obtained from the lamellae indicate that the chain axis is normal to the surface of the crystal and the chain must exit the top surface of the crystal, fold and re-enter. The exact nature

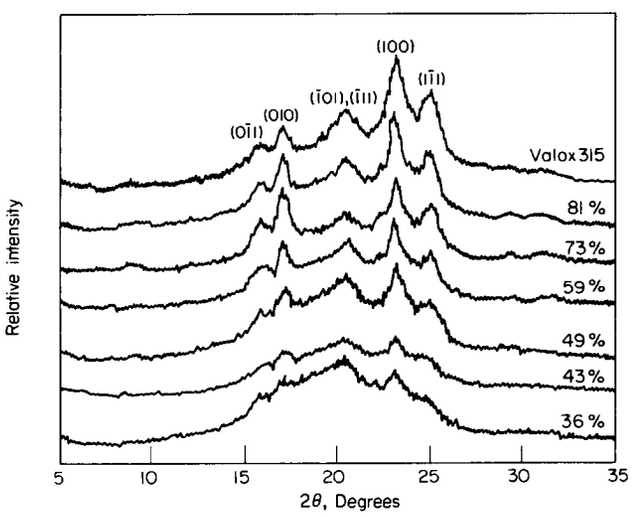

Figure 11 WAXS scans of the series of polyether–polyesters of various compositions

Table 2 (100)1(010) and (011) unit cell spacings of polyether-polyesters as a function of hard segment content as measured by WAXS (nanometers)

Wt% 4GT	d_{100}	d_{010}	$d_{0\bar{1}1}$	T_c °C
100%	0.382	0.517	0.557	220
81%	0.383	0.517	0.556	210
73%	0.383	0.516	0.555	200
59%	0.383	0.517	0.559	195
49%	0.383	0.516	0.558	190
Calculated*	0.382	0.514	0.550	

* Based on the unit cell presented by Desborough and Hall[27]

of the type of folding, i.e. adjacent re-entry *versus* random switchboard, cannot be determined. Indeed, the specifics of chain folding are still debated for homopolymers[33]. Nevertheless, some pertinent comments can be made. Small-angle X-ray studies in the literature indicate that PTMEG/4GT polyether–polyesters exhibit the classical dependence of the long period on crystallization temperature[2]. At high crystallization temperatures thicker lamellae are formed. The aspect different from homopolymer behaviour is that the crystal growth in these copolymers is limited by the number of hard segment sequences available that are long enough to traverse the stable crystal thickness at a given T_c which, in turn, is determined by the sequence distribution. This implies that most of the hard segment sequences participating in the crystal core must terminate with a soft segment sequence near the surface of the lamella. Only the longest hard segment sequences in the distribution would be of sufficient length to undergo tight folding and traverse the crystal twice. The evidence presented by Seymour *et al.* on etching of the fold surfaces and subsequent g.p.c. experiments indicated that there was a fraction of stems twice the crystal thickness demonstrating that some of the longest sequences may indeed fold tightly. The fold surface must consist of mainly soft segment molecules and short hard segment sequences. The thickness of the amorphous layer (fold surface) should be directly proportional to the soft segment content of the sample. The disparity in length of the sequences participating in crystallization naturally leads one to expect relatively diffuse crystal boundaries. Yet, as mentioned earlier, SAXS studies of the interface have indicated relatively sharp boundaries[9].

Strobl *et al.* have presented a model for the crystallization of low density polyethylene where crystal growth is not directly controlled by the sequence distribution of chain lengths between branch points but by the amorphous layer between growing lamellae[34]. In low density polyethylene the long branches are excluded from the crystals to the fold surfaces and interlamellar regions. The model was postulated to explain the strong (reversible) temperature dependence of the long period while accounting for a relatively constant crystal core thickness. It appears unlikely that the polyether–polyesters studied in this work follow this model. The fact that the lamellae observed in this study and the hedrites examined by Zhu *et al.* stop growing many microns apart suggests that depletion of the long hard segment sequences controls the crystallization. It is not known whether polyether–polyesters exhibit a temperature dependent long period or crystal thickness, although it is reasonable to predict that it would be observed.

It is striking that single crystals of a random block copolymer can be grown from the melt. Lotz *et al.* have reported, similar to this work, that it is actually easier to grow single crystals of a diblock copolymer of polyethylene oxide (PEO) with polystyrene (PS) than from PEO homopolymer[35]. The PEO/PS crystals were essentially identical to hompolymer PEO crystals with the PS being confined to the fold surface. Single crystals of short branched polyethylene[36] and of copolymers of tetramethyl-*p*-silphenylene siloxane/dimethylsiloxane[37,38] have also been reported. In contrast, in both of these latter cases the copolymers did not form individual single crystals as readily as the homopolymers.

CONCLUSIONS

Single crystals of 4GT have been grown in thin films from the melt of random block copolymers based on PTMEG/4GT. Well defined lamellae have been observed in films down to 49 wt% (0.83 mole fraction) 4GT component. Electron diffraction and WAXS support a model of a relatively pure 4GT crystal core in the α form with the PTMEG sequences and short hard segments rejected to the crystal fold surface and soft segment rich matrix. This is good agreement with the models presented previously by Cella[1,4,5] and Seymour *et al.*[6] with additional insight into the fine details of the morphology. The strong (*hk*0) diffraction pattern exhibited by the lamellae indicates the ç axis is normal to lamellar surface and the polymer chains must undergo some type of chain folding.

The crystallization behaviour indicates that the lateral dimensions of the crystal growing at a given temperature are controlled by the number of 4GT sequences long enough to traverse the crystal which is determined by the sequence distribution. This leads to an initial population of crystals formed at T_c and a second set of small crystals that grow upon cooling to room temperature. The result is fractionation by sequence length due to coupling of the sequence distribution with the stable crystal size at T_c.

ACKNOWLEDGEMENT

The authors would like to acknowledge the National Science Foundation for financial support (grant CPE-8118232) and the Materials Research Laboratory at the University of Massachusetts for the use of the experimental facilities.

REFERENCES

1 Cella, R. J. *J. Polym. Sci., Symp.* 1973, **42**, 737
2 Wegner, G., Fujii, T., Meyer, W. and Lieser, G. *Die Angew. Makromol. Chem.* 1978, **74**, 295
3 Lilaonitkal, A. and Cooper, S. L. *Rubber Chem. Technol.* 1977, **50**, 1
4 Cella, R. J. 'Encyclopedia of Polymer Science and Technology', Supplement Vol. 2, Wiley and Sons, 1977, p. 485
5 Buck, W. H., Cella, R. J., Gladding, E. K. and Wolfe, J. R. *J. Polym. Sci. Symposium* 1974, No. **48**, 47
6 Seymour, R. W., Overton, J. R. and Corley, L. S. *Macromolecules* 1975, **8**, 331
7 Zhu, L.-L. and Wegner, G. *Makromol. Chem.* 1981, **182**, 3625
8 Zhu, L.-L., Wegner, G. and Bandara, U. *Makromol. Chem.* 1981, **182**, 3639
9 Bandara, U. and Droscher, M. *Colloid Polym. Sci.* 1983, **261**, 26
10 Siemann, U. and Ruland, W. *Colloid Polym. Sci.* 1982, **269**, 999
11 Hashimoto, T., Todo, A., Itoi, H. and Kawai, H. *Macromolecules* 1977, **10(2)**, 377
12 Wistsiepe, W. K. and Hoeschele, G. K. *Angew. Makromol. Chem.* 1973, **29–30**, 267
13 Shih, C. K. and McKenna, J. M., submitted to *Rubber Chem. Technol.*
14 Wolfe, Jr., J. R. *Rubber Chem. Technol.* 1977, **50(4)**, 688
15 Shih, C. K., to be submitted to *Rubber Chem. Technol.*
16 Low, A., Vesley, D., Allen, P. and Bevis, M. *J. Mater. Sci.* 1979, **14**, 1109
17 Sherman, E. S. and Thomas, E. L. *J. Mater. Sci.* 1979, **14**,1109
18 Sherman, E. S., Adams, W. W. and Thomas, E. L. *J. Mater. Sci.* 1981, **16**, 1
19 Chacko, V. P., Adams, W. W. and Thomas, E. L. *J. Mater. Sci.* 1983, **18**, 1999
20 Wunderlich, B. 'Macromolecular Physics', Vol. 1, Academic Press, N.Y., 1973, p. 217
21 Shih, C. K., DuPont Co., unpublished data
22 Briber, R. M. *PhD Dissertation*, Polymer Science and Engineering, University of Massachusetts, 1984
23 Jakeways, R., Ward, I. M., Wilding, M. A., Hall, I. H., Desborough, I. J. and Pass, M. R. *J. Polym. Sci., Polym. Phys. Edn.* 1975, **13**, 799
24 Mencik, Z. *J. Polym. Sci., Polym. Phys. Edn.* 1975, **13**, 2173
25 Yokouchi, M., Sakakibara, Y., Chatani, Y., Tadokoro, H., Tanaka, T. and Yoda, K. *Macromolecules* 1976, **9**, 266
26 Hall, I. H. and Pass, M. G. *Polymer* 1976, **17**, 807
27 Desborough, I. J. and Hall, I. H. *Polymer* 1977, **18**, 825
28 Briber, R. M. and Thomas, E. L., submitted to *Polymer*
29 Thomas, E. L. *J. Mater. Sci.* 1977, **12**, 234
30 Boudet, A. and Kubin, L. D. *J. Microsc. Spectrosc. Electron.* 1980, **5**, 187
31 Khoury, F. A., private communication
32 Illers, K. H. *Colloid. Z. Z.* 1980, **258**, 117
33 Faraday Discussions of the Royal Society, *Organization of Macromolecules in the Condensed Phase*, 1979, **68**
34 Strobl, G. R., Schneider, M. J. and Voight-Martin, I. G. *J. Polym. Sci., Polym. Phys. Edn.* 1980, **18**, 1361
35 Lotz, B., Kovacs, A. J., Bassett, G. A. and Keller, A. *Kolloid Z. Z. Polym.* 1966, **209**, 115
36 Geil, P. H. 'Polymer Single Crystals', Krieger Publishing Co., N.Y., 1973, p. 100
37 Li, H. M. and Magill, J. H. *J. Polym. Sci., Polym. Phys. Edn.* 1978, **16**, 1059
38 Kojima, M. and Magill, J. H. *J. Macromol. Sci.-Phys.* 1974, **B10(3)**, 419